RSC Advances

ROYAL SOCIETY OF CHEMISTRY

www.rsc.org/advances

TOC

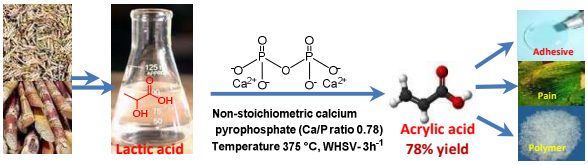

Lactic acid dehydration using non-stoichiometric calcium pyrophosphate catalyst (Ca/P ratio 0.78) has resulted in 78% acrylic acid yield due to formation of calcium lactate as an intermediate on catalyst surface.

Cite this: DOI: 10.1039/c0xx00000x

www.rsc.org/xxxxxx

ARTICLE TYPE

Nonstoichiometric Calcium Pyrophosphate: Highly Efficient and Selective Catalyst for Dehydration of Lactic Acid to Acrylic Acid

Vidhya C. Ghantani,[a,b] Mohan K. Dongare[†*a] and Shubhangi B. Umbarkar*[a,b]

Received (in XXX, XXX) Xth XXXXXXXXX 20XX, Accepted Xth XXXXXXXXX 20XX

DOI: 10.1039/b000000x

Calcium phosphate catalysts were prepared by co-precipitation method using calcium nitrate and mixture of ammonium and different sodium phosphates as calcium and phosphate precursors respectively. Depending on the phosphate precursor the pH of the synthesis mixture changed during the catalyst precipitation. The catalysts characterisation by XRD and ICP revealed the formation of calcium pyrophosphate structure with varying Ca/P ratio from 1.02 to 0.76 which could be correlated to the different pH of the synthesis solution. Vapour phase dehydration of lactic acid to acrylic acid was carried out using these calcium pyrophosphate catalysts. Non-stoichiometric calcium pyrophosphate catalyst with Ca/P ratio 0.76 was found to be the most efficient catalyst among synthesized series with 100% lactic acid conversion and 78% acrylic acid selectivity at 375 °C. The higher selectivity for acrylic acid has been correlated to the increased acidity and reduced basicity of non-stoichiometric calcium pyrophosphate compared to other stoichiometric pyrophosphates. *In situ* FTIR studies showed the formation of higher amount of calcium lactate on non-stoichiometric compared to stoichiometric pyrophosphate leading to higher selectivity for acrylic acid.

Introduction

Depletion of fossil fuels and increasing pollution due to greenhouse gases emitted in the atmosphere has forced researchers worldwide to develop clean technologies based on renewable raw materials for sustainable development. Sustainable production of fuels and chemicals is possible using lignocellulosic biomass as an attractive raw material. Lactic acid derived from biomass fermentation has been identified as one of the high potential platform chemical in the biomass economy.[1,2] Lactic acid is very reactive molecule due to the presence of active functional groups, -OH and -COOH, which can be used to convert lactic acid to many value added products such as acrylic acid, propionic acid[3], 2,3-pantanedione[4], acetaldehyde[5], pyruvic acid[6], 1,2 propane diol[7] by different pathways. Acrylic acid, its amides and esters find wide applications in surface coatings, textiles, adhesives, paper treatment, leather, fibres, detergents, polymeric flocculants, dispersants, paints, adhesives, binders for leather, and in acrylate polymers etc. Dehydration of lactic acid to acrylic acid is being considered as one of the attractive alternate route for the manufacture of acrylic acid from renewable raw materials.

Catalytic dehydration of lactic acid /lactates to acrylic acid/acrylates has been reported previously using inorganic salts such as phosphates, silicates, carbonates, nitrates and sulphates as catalysts.[8,9,10,11,12] Catalysts having strong acidity mainly show decarbonylation/decarboxylation of lactic acid to acetaldehyde.[5] Hence for zeolites, modifiers such as potassium nitrate, lanthanum oxide and alkali phosphates as well as various alkaline earth metals like Ca, Mg, Sr, Ba etc. were used to change the surface acidity to achieve high efficiency for selective dehydration of lactic acid to acrylic acid.[13] Previously various phosphate based catalysts like sodium dihydrogen phosphate (NaH_2PO_4), $Ca_3(PO_4)_2$ supported on silica, silica/alumina, aluminium phosphate and Na_2HPO_4 in supercritical water, were used for lactic acid dehydration.[14] However some of the modifiers leach out easily from the support during reaction leading to catalyst deactivation. Hence water insoluble salts with desirable acidity were employed in the dehydration of lactic acid. Various alkali phosphates (ortho and pyro) such as calcium, strontium and barium phosphates were used for lactic acid dehydration by Blanco *et al*.,[15] with maximum acrylic acid selectivity of only 49% using $Ba_3(PO_4)_2$. Peng and co-workers investigated the effect of acidity of various metal sulfates on lactic acid dehydration, and $BaSO_4$ showed 74% selectivity for acrylic acid due to moderate acidity.[16] When mixture of $Ca_3(PO_4)_2$ and $Ca_2P_2O_7$ (50/50 wt.%) was tested for dehydration of ethyl lactate, methyl lactate and lactic acid, the conversion increased in the order ethyl lactate<methyl lactate< lactic acid, however the selectivity for acrylic acid was observed in the reverse order.[17] Matsuura and co-workers studied hydroxyapatite with different cations and anions for lactic acid dehydration and results showed calcium and strontium hydroxyapatite with moderate acidity to give highest acrylic acid yield. The same group studied addition of different bases like NaOH and ammonia for adjusting the pH and formation of non-stoichiometric calcium hydroxyapatite with incorporation of sodium which resulted in 78% yield for acrylic acid using 38% lactic acid solution with very low WHSV.[18] Similarly hydroxyapatite with Ca/P ratio of 1.62, calcined at 360

°C has shown 71% acrylic acid selectivity with 70% lactic acid conversion.[19] Normally different lactic acid concentrations ranging from 20wt% to 40wt% were used for lactic acid dehydration with lower WHSV leading to low space time yield.

Lactic acid dehydration requires catalysts with weak acidity and weak basicity, however fine tuning of surface acidity and basicity is very important for achieving maximum selectivity for acrylic acid. Recently we have reported lactic acid dehydration using series of hydroxyapatite with different Ca/P ratio as catalyst.[20] The catalyst with minimum Ca/P ratio of 1.5 showed maximum efficiency with 100% conversion and 60% acrylic acid selectivity along with the formation of acetaldehyde as the only byproduct. The catalyst with Ca/P ratio 1.5 showed the required acid base balances to achieve acrylic acid selectivity of 60%. As Ca/P ratio of hydroxyapatite was decreased from 1.67 (stoichiometric) to 1.5, considerable improvement in acrylic acid selectivity was observed. Hence to further increase the acrylic acid selectivity, the calcium phosphate catalysts were prepared using modified synthetic procedure to decrease the Ca/P ratio further using mixture of diammonium hydrogen phosphate and sodium phosphates as phosphate precursor and without maintaining constant pH throughout the catalyst preparation and the results are reported herein.

Results and Discussion

A series of calcium phosphate (CP) catalysts were prepared using calcium nitrate, diammonium hydrogen phosphate and additional phosphate precursors like $NaH_2PO_4.2H_2O$, $Na_2HPO_4.2H_2O$ and $Na_3PO_4.12H_2O$ to tune the Ca/P ratio by increasing the phosphate content. It is known that preparation of calcium phosphates is very sensitive to pH of the precursor solution and drastically affects the Ca/P ratio of the final catalyst composition. During the synthesis of catalysts using sodium phosphates, the pH of $Ca(NO_3)_2$ and $(NH_4)_2HPO_4$ was adjusted to 8. However due to difference in pH of the aqueous solution of sodium phosphate precursors, the pH of the mixed phosphate solution was different (Table 1). Hence during addition of calcium nitrate solution to phosphate mixture and ultimately precipitation of calcium phosphate the pH of the mixture gradually decreased reaching 6 after complete addition of calcium nitrate. Hence the change in the pH of the solution during precipitation is expected to affect the catalyst structure, Ca/P ratio and in turn the catalytic activity. The pH of the sodium precursors are given in Table 1. Hence for comparison one catalyst was prepared without using any sodium phosphate and denoted as CP. For this catalyst also the pH of the synthesis mixture decreased from 8 to 6 after complete precipitation.

The bulk and surface Ca/P ratio was determined by ICP and EDAX analysis and results are shown in Table 2. The Ca/P ratio for CP-1 and CP-2 were found to be 1.04 and 1.09 respectively which is in accordance with the almost similar pH of the combined phosphate solution. However for CP-3 the Ca/P ratio decreased considerably to 0.76. The catalyst prepared without sodium phosphate showed higher Ca/P ratio of 1.27.

At different pH different phosphate species exist, and at pH 8 predominantly HPO_4^{-2} exists.[21] HPO_4^{-2} species has very high affinity for calcium leading to precipitation of $CaHPO_4$. The precipitation of calcium phosphate from calcium and phosphate solutions is a pH controlled process. At lower pH the solubility of calcium phosphate increased leading to the decrease in calcium incorporation, which in turn decreases the Ca/P ratio.[22] Addition of sodium phosphates led to increase in phosphate concentration thus resulting in decrease in Ca/P ratio. The additional phosphate alters the equilibrium between PO_4^{-3} to HPO_4^{-2} to $H_2PO_4^{-1}$ which leads to the further decrease in Ca/P ratio. It was reported that Ca/P ratio of the precipitate does not depend directly on the Ca/P ratio of initial reagents of calcium and phosphate but depends on pH and temperature during precipitation.

Table 1. pH of the phosphate solution during precipitation.

Catalyst	Phosphate precursor	pH of Na-phosphate solution	pH of combined phosphate solution	pH of solution after complete precipitation
CP-1	$NaH_2PO_4.2H_2O$	4	7	5
CP-2	$Na_2HPO_4.2H_2O$	8.5	7.5	5
CP-3	$Na_3PO_4.12H_2O$	12	10	5
CP	-	-	-	5

The surface area of all the catalysts determined using the BET method was found to be in the range 21-29 m^2/g as shown in Table 2.

Table 2. Textural characterization, acidity and basicity of calcium pyrophosphates.

Catalyst Name	Surface area, m^2/g	CO_2 desorbed, µmol/g	NH_3 desorbed, µmol/g	Acid Base Balance	Ca/P ratio by ICP	Ca/P ratio by EDAX
CP-1	29	17.054	114	7	1.04	1.02
CP-2	21	16.094	128	8	1.09	1.03
CP-3	29	15.317	167	11	0.76	1.08
CP	28	34.907	071	2	1.27	1.10

The change in pH during spontaneous precipitation of calcium phosphate from supersaturated solutions was studied at 30°C, stirring speed 700 rpm and shown in Fig. S1. It showed decrease in pH during the first few minutes, followed by an irregular and slow decrease and finally became stable after 2 h.

The powder X-ray diffraction (XRD) patterns of synthesized catalysts are shown in Fig. 1. The XRD pattern showed the crystalline nature for all the catalysts. The diffraction peaks at 26.7, 27.7, 28.9, 29.3, 30.69 and 32.37º match with the structure of β calcium pyrophosphate (JCPDS-33-0297). The intensity of the peak at 29.3º considerably decreased in CP-3 compared to remaining catalysts indicating structural distortion which may be due to calcium deficiency as observed by EDAX and ICP analysis. However the overall XRD pattern retains the β-pyrophosphate structure. As the Ca/P ratio for CP-3 is considerably low compared to pyrophosphate structure (Ca/P =1) the XRD of as synthesised catalyst was recorded (denoted as CP-3* in Fig. 1). The peaks at 26.38°, 30.15°, 32.52°, 35.82°, 49.26°, 53.02° matched with monetite structure of $CaHPO_4$ (monetite JCPDS-04-0513) which transformed to pyrophosphate after calcinations. Skinner[23] has studied the conversion of $CaHPO_4$ to different forms of calcium pyrophosphates at different temperatures and showed the formation of β calcium pyrophosphate to be at the temperature below 800 °C. As all the

catalysts in the present work were calcined at 600 ºC the formation of stable β-pyrophosphate was observed in accordance with literature reports. In Ca-pyrophosphate or monetite structure the theoretical Ca/P ratio is 1 which is matching with Ca/P ratio in CP-1 and CP-2, however for CP-3 the ratio is considerably low (0.76) indicating non-stoicheometric or Ca deficient pyrophosphate structure. The only reported calcium phosphate with lower Ca/P ratio of 0.5 are $Ca(H_2PO_4)_2$, monocalcium phosphate monohydrtated (MCPM) or anhydrous monocalcium phosphate (MCPA), which are water soluble and stable only in extremely acidic pH of 0-2. Hence in the present work we could precipitate the calcium phosphate with lower Ca/P ratio in basic medium as well as retain the pyrophosphate structure at high temperature with calcium deficiency.

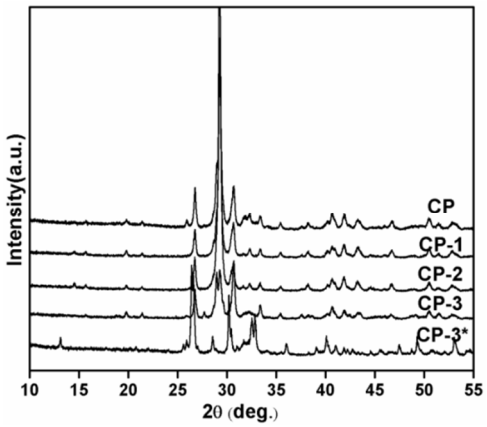

Fig.1 The powder X-ray diffraction (XRD) patterns of synthesized catalysts, CP-3*- as synthesised CP-3 catalyst.

The acid base properties of the catalysts were evaluated by temperatures programmed desorption (TPD) of NH_3 (Fig. S2) and CO_2 (Fig. S3) and the results are shown in Table 2. As the Ca/P ratio decreased from CP, CP-1 to CP-3, there is decrease in basicity and increase in the acidity. Phosphate groups in catalyst are responsible for acidity whereas Ca^{2+} ions are responsible for the basicity. Hence increase in the basicity and decrease in the acidity was observed as expected with increase in the Ca/P ratio.[20] CP-3 catalyst showed the highest acidity. The basicity of the reported CP catalyst was very weak (expressed in µmol/g) and the TPD profile is shown in Fig. S3.

Catalyst structure was further confirmed by FTIR spectroscopy (Fig. 2). Typical pyrophosphate stretching and bending vibrations were observed at 1215-941 and 723 cm^{-1} respectively.[24] Bands at 613–494 cm^{-1} are assigned to phosphate bending vibrations.[25] Thus the β calcium pyrophosphate formation was confirmed by both XRD and FTIR studies. Likewise the formation of $CaHPO_4$ in as synthesised CP-3 catalyst (CP-3*) was also confirmed by FTIR from the characteristic band for HPO_4^{-1} at 898 cm^{-1}.

Raman analysis showed the presence of monoclinic β-calcium pyrophosphate (Fig. 3). The Raman peaks at 1159, 1115, 1049, 736, 524, 356 and 355 cm^{-1} matched with the Raman peaks reported for monoclinic calcium pyrophosphate.[26] The particle size of all the CP catalyst was determined using SEM and the images are given in Fig. S4. However there was no considerable difference in particle size was observed.

Thus the structure of all the synthesised catalysts was confirmed to be β-calcium pyrophosphate.

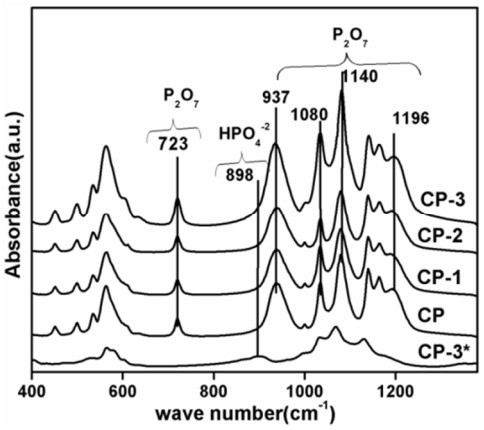

Fig. 2 FTIR spectra of synthesized CP catalysts and as synthesized CP-3 catalyst.

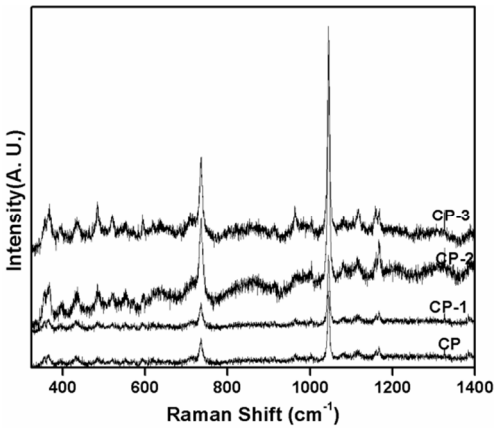

Fig. 3 Raman spectra of synthesized CP catalysts.

Catalytic activity

The synthesized calcium phosphate (CP) catalysts were tested for vapour phase dehydration of lactic acid (scheme 1) and the results are shown in Table 3. The reaction was carried out with the previously reported optimised reaction conditions[20] *i. e.* using 50% (w/w) aqueous solution of lactic acid with WHSV of 3 h^{-1} at 375 ºC. As expected 100% lactic acid conversion was obtained with all CP catalysts at 375 ºC using 50% lactic acid solution though with variable acrylic acid selectivity. CP-3 catalyst showed maximum selectivity of 74% for acrylic acid compared to CP-2 (70%), CP-1 (68%) and CP (55%). As CP-3 catalyst showed highest selectivity for acrylic acid, the effect of different reaction parameters such as temperature, residence time, concentration on lactic acid dehydration was studied using CP-3 catalyst and the results are given in Table 4.

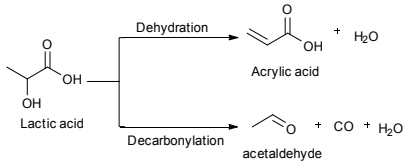

Scheme 1 General schematic for lactic acid conversion to acrylic acid and acetaldehyde.

Table 3: Dehydration of lactic acid to acrylic acid using calcium phosphate with different Ca/P ratio.

Sl. no	Catalyst	Conv.	Acrylic Acid Selectivity	Acetaldehyde Selectivity	Other products Selectivity
1	CP	100	55	30	15
2	CP-1	100	68	15	17
3	CP-2	100	70	13	17
4	CP-3	100	74	10	16

Reaction condition: carrier gas- N_2, carrier gas flow-15 mL min^{-1}, WHSV 3 h^{-1}, lactic acid conc.- 50% (w/w), temperature- 375 °C, other products- propanoic acid, 2,3-pentanedione, CO, CO_2.

Effect of temperature

The effect of temperature on lactic acid conversion and acrylic acid selectivity was studied by varying the temperature from 325 to 400 ºC (Table 4, entry 1). Conversion of lactic acid increased from 75 to 100% with increase in reaction temperature from 325 to 400 °C with 50% lactic acid concentration and WHSV of 3 h^{-1}. Initially increase in the acrylic acid selectivity was observed from 32 to 74% with increase in the temperature from 325 to 375 ºC, however further increase in the temperature to 400 ºC led to decrease in the acrylic acid selectivity to 60% with corresponding increase in the formation of acetaldehyde and polylactates. At 325 ºC lowest lactic acid conversion and acrylic acid selectivity was observed due to lactide formation.

Effect of residence time

The residence time of lactic acid on CP-3 was varied by progressively changing the WHSV from 1 to 4.5 h^{-1}. When WHSV was increased from 1 to 3 h^{-1}, the lactic acid conversion remained at 100% however with further increase in WHSV to 4 and 4.5 h^{-1}, the conversion decreased to 90 and 85% respectively due to decrease in residence time (Table 4, entry 2). Whereas volcano type trend was obtained for acrylic acid selectivity. The acrylic acid selectivity increased from 54% to 74% with increase in WHSV from 1 to 3 h^{-1} and then it decreased to 68 and 65% with further increase in WHSV to 4 and 4.5 h^{-1} respectively. As the residence time decreased there was increase in selectivity, though with 100% conversion for lactic acid. At very low residence time (WHSV-4, 4.5) there was decrease in conversion of lactic acid as well as selectivity for acrylic acid. WHSV-3 h^{-1} provides optimum residence time for maximum conversion as well as acrylic acid selectivity on CP-3 catalyst.

Effect of lactic acid concentration

The lactic acid concentration was gradually increased from 25 to 80 wt% (wt/wt aqueous solution) to study its effect especially on acrylic acid selectivity (Table 4, entry 3). Complete lactic acid conversion (100%) was obtained with 25 and 50% lactic acid concentration however gradual increase in the lactic acid concentration to 80% led to decrease in lactic acid conversion to 70%. Maximum selectivity (78%) for acrylic acid was obtained when 25% lactic acid was used which steadily decreased to 53% with increase in the lactic acid concentration to 80%. Acrylic acid yield of 78% is the highest yield reported so far in the literature for lactic acid dehydration at very high WHSV (3 h^{-1}). With increase in the lactic acid concentration residence time decreased which led to the decrease in Ca-lactate formation and consequently increase in the decarbonylation leading to more formation of acetaldehyde. It is worth mentioning that mass balance for all the above mentioned reaction was 85-90%. Catalyst stability of CP-3 was tested under optimised reaction conditions and the catalytic activity was stable upto 20 h. The acetaldehyde formed in all the above mentioned reaction was predominantly due to decarbonylation of lactic acid as confirmed by GC analysis however formation of CO_2 was also observed with less selectivity indicating lesser extent of decarboxylation compared to decarbonylation. Decarboxylation of lactic acid is associated with formation of hydrogen which may be responsible for propionic acid formation by hydrogenation of acrylic acid. Alternate pathway for formation of propionic acid is deoxygenation of lactic acid. However hydrogenation of acrylic acid is more feasible path for formation of propionic acid as per previous studies.[27] Deoxygenation of lactic acid has been studied before in the literature. Previous studies have shown deoxygenation of lactic acid in presence of acidic catalysts like hydriodic acid[28], supported heteropoly acids,[5] supported nitrates and phosphates,[4a,4b,29,30] as well as doped zeolites[13a] or platinum based catalyst under high hydrogen pressure.[31] Various homogenous catalysts (Pd, Pt or Ir complexes) also have been used for deoxygenation of lactic acid in water at lower pH.[27,32] However in the present work the catalyst is very weakly acidic as well as reaction conditions are totally different than typically required for deoxygenation of lactic acid. Hence the formation of propionic acid in present work would be due to hydrogenation of acrylic acid and not by deoxygenation of lactic acid.

Table 4: Effect of various parameters on dehydration of lactic acid to acrylic acid using CP-3 catalyst.

Entry	Reaction parameters		% Conv.	% Acrylic acid Selectivity	% Acetaldehyde Selectivity	% Other products Selectivity
1	Temp.[a] (°C)	325	75	32	15	53[#]
		350	90	45	15	40
		375	100	74	10	16
		400	100	60	20	20
2	WHSV[b] (h^{-1})	1	100	54	22	24
		2	100	62	16	22
		3	100	74	10	16
		4	90	68	12	20
		4.5	85	65	18	17
3	Lactic acid conc.[c] (w/w%)	25	100	78	8	14
		50	100	74	10	16
		60	96	60	20	20
		70	80	58	20	22
		80	70	53	23	24

Reaction conditions: Catalyst- CP-3, carrier gas- N_2, carrier gas flow-15 mL min^{-1} [a]: WHSV- 3 h^{-1}, Lactic acid conc.- 50% (w/w) [b]: Lactic acid conc.- 50% (w/w), Temp- 375 °C [c]: Temp- 375 °C, WHSV- 3 h^{-1} and other products- propanoic acid, 2,3-pentanedione, CO, CO_2, # lactide.

Recently many phosphate based catalysts such as $Ba_3(PO_4)_2$,[15] Na_2HPO_4 supported on NaY,[33] calcium and strontium hydroxyapatites[18a] as well as non-stoichiometric calcium hydroxyapatite modified with sodium[18b] have been used for lactic acid dehydration to acrylic acid. All the above mentioned phosphate based catalysts were operated in the temperature range of 340-400 ºC with lactic acid concentration of 20-40%. Among the phosphate based catalysts Na_2HPO_4/NaY showed maximum lactic acid conversion of 93.5% with 79.5% selectivity for acrylic

acid. Zhang *et al.*[34] have studied lactic acid dehydration using $NaNO_3$/SBA-15 catalyst with almost complete conversion, however with very poor (42%) acrylic acid selectivity. When $BaSO_4$ was used for lactic acid dehydration at 400 ºC using 20% lactic acid solution, almost 100% lactic acid conversion is reported with 66% selectivity for acrylic acid.[16] Lactic acid dehydration on different barium phosphates was screened, however only barium pyrophosphate $Ba_2P_2O_7$ has shown very high acrylic acid selectivity (76%) with 20wt% lactic acid concentration and with considerably lower WHSV (flow rate 1ml/h) compared to present work.[35] Compared to previous reports on lactic acid dehydration to acrylic acid, the results obtained in the present study are better with 100% conversion and 78% acrylic acid selectivity. Especially the use of high concentration of lactic acid and very high WHSV leading to high per pass yield are the major advantages of the present catalysts.

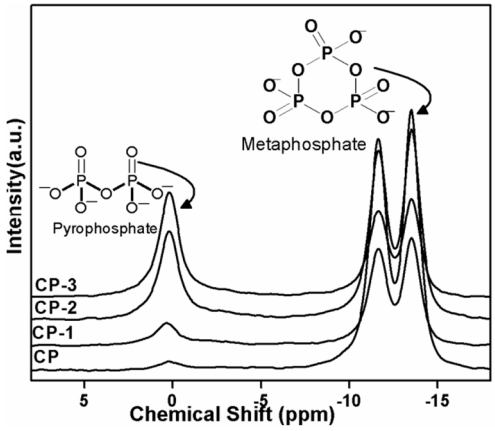

Fig. 4 ^{31}P mass NMR spectra a. CP b. CP-1, c. CP-2 and d.CP-3.

Though all the synthesised CP catalysts have shown β-calcium pyrophosphate structure, only CP-3 catalyst has shown maximum selectivity for acrylic acid whereas CP has shown lowest acrylic acid selectivity. Hence the structure of all CP catalysts was further studied by ^{31}P-NMR spectroscopy (Fig. 4 and Fig. S5). The NMR spectra showed three isotropic peaks at 0.2(Q^0), -11.65(Q^1) and -13.51(Q^1) ppm. Q^0 represents the pyrophosphate species and Q^1 represents the metaphosphate species (as shown in Fig. 4).[36] The intensities of different species in CP showed the concentration of pyrophosphate species (Q^0 peak at 0.2 ppm) to be less than metaphosphate species (Q^1 peak at -11.65 and -13.51 ppm). In CP-3 the concentration of pyrophosphate species was considerably higher compared to metaphosphate species. The intensity of pyrophosphate peak gradually increased from CP to CP-3 which may be correlated to the acrylic acid selectivity which also gradually increased from CP to CP-3. The Ca/P ratio changed from 1.27 to 0.76 for CP and CP-3. More terminal P-OH groups are present in pyrophosphate species compared to metaphosphate species as shown in the structure in Fig. 4, which is in accordance with higher acidity of CP-3 compared to CP.

As per the proposed mechanism in our previous work on lactic acid dehydration, calcium lactate formation is crucial for acrylic acid selectivity. To check the formation of calcium lactate species, *in-situ* FTIR studies were carried out using previously reported experimental conditions[20] on catalysts which showed minimum (CP) and maximum (CP-3) selectivity for acrylic acid. Lactic acid was adsorbed on CP and CP-3 at room temperature and physisorbed lactic acid was removed by drying the catalyst at room temperature for 8 h and the FTIR spectrum was recorded. Further, the adsorbed lactic acid was desorbed at 50, 100 and 150 °C. The difference spectra of CP and CP-3 at 150 °C are shown in Fig. 5. Calcium lactate formation on both the catalysts CP and CP-3 was confirmed by carbonyl peak at 1600 cm^{-1} whereas free lactic acid adsorbed on catalyst was confirmed by presence of carbonyl peak at 1748 cm^{-1}. Carbonyl peaks of calcium lactate and lactic acid were used as measure of extent of calcium lactate formation which in turn can be correlated to the selectivity for acrylic acid observed on particular catalyst. The ratio of area of the carbonyl peak at 1600 (for calcium lactate) and at 1748 cm^{-1} (for lactic acid) was calculated for CP and CP-3. The ratio was considerably higher for CP-3 (0.583) compared to CP (0.350) indicating higher extent of calcium lactate formation on CP-3 compared to CP which can be directly correlated to higher selectivity for acrylic acid observed on CP-3 compared to CP.

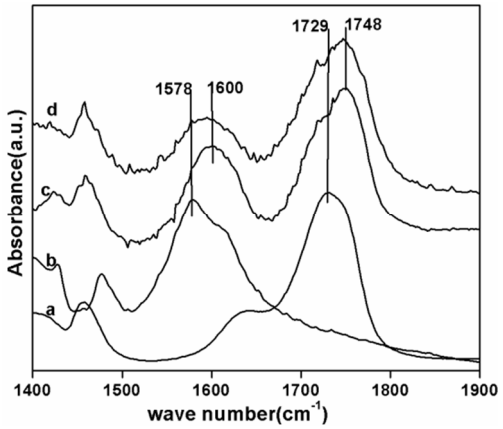

Fig. 5 FTIR spectrum of (a) lactic acid (b) calcium lactate from FTIR database, FTIR difference spectra of lactic acid adsorbed (c) CP-3, (d) CP at 150 °C.

Though Ca/P ratio is less for CP-3 compared to CP the more formation of calcium lactate is observed on CP-3 which may indicate the more availability of calcium on the surface for formation of calcium lactate in CP-3 which may be due to the structural features of CP-3.

Conclusion

Non stoichiometric calcium pyrophosphate catalyst prepared with Ca/P ratio 0.76 prepared by modifying synthetic procedure using mixture of diammonium hydrogen phosphate and sodium phosphates as phosphate precursors. This catalyst has shown very high efficiency for vapour phase dehydration of lactic acid to acrylic acid with 100% conversion and 74% acrylic acid selectivity at 375 ºC with WHSV of 3 h^{-1} using 50% lactic acid concentration. The acrylic acid selectivity was further improved to 78% with 25% lactic acid concentration. The higher selectivity for acrylic acid was attributed to acid base balance at lower Ca/P ratio leading to formation of higher amount of calcium lactate as an intermediate compared to other stoichiometric calcium pyrophosphates as evidenced by in situ FTIR studies.

Experimental Section

Materials

Calcium nitrate, di-ammonium hydrogen phosphate, ammonium hydroxide solution, sodium hydrogen phosphate ($NaH_2PO_4.2H_2O$), disodium hydrogen phosphate ($Na_2HPO_4.2H_2O$), and tri sodium phosphate ($Na_3PO_4.12H_2O$) were obtained from Thomas Baker chemicals India Ltd. Lactic acid (89%) was obtained from our CSIR-National Chemical Laboratory (CSIR-NCL) Pune pilot plant which is obtained from sugarcane fermentation process (process developed by CSIR-NCL).

Catalyst preparation method

Calcium phosphates catalysts using calcium nitrate, diammonium hydrogen phosphate and sodium phosphates were prepared by precipitation method. Typical sodium phosphate precursors like $NaH_2PO_4.2H_2O$, $Na_2HPO_4.2H_2O$ and $Na_3PO_4.12H_2O$ were used for the preparation and the final catalysts were denoted as CP-1, CP-2 and CP-3 respectively. In a typical synthesis of CP-1, calcium nitrate (36.95 g) and diammonium hydrogen phosphate (13.8 g) were dissolved separately in 125 mL deionised water each. Initially the pH of both the solutions was adjusted to 8 by addition of ammonium hydroxide solution (5% aqueous). $NaH_2PO_4.2H_2O$ (3.39 g) dissolved in 25 mL deionised water was added to the diammonium hydrogen phosphate solution. Calcium nitrate solution was added drop wise to the above mixture of phosphate precursors with constant stirring (700rpm) at room temperature. As the precipitation proceeds decrease in pH was observed. A thick white precipitate formed was aged for 12 h then filtered, washed with water and dried in an oven at 120 ºC for 12 h. The dried catalyst was calcined at 600 ºC for 4 h. Catalysts CP-2 ($Na_2HPO_4.2H_2O$ 1.911 g) and CP-3 ($Na_3PO_4.12H_2O$ 2.7 g) were prepared following the similar procedure as mentioned above except the source of sodium phosphate. Calcium phosphate catalyst without sodium phosphate was prepared for comparison, with Ca/P ratio 1.5 and denoted as CP. For preparation of CP calcium nitrate (38.9 g) and diammonium hydrogen phosphate (14.5 g) solutions were prepared separately in deionised water (125 mL each). Initially the pH of both the solutions was adjusted to 8 by adding ammonium hydroxide solution (5% aqueous). Calcium nitrate solution was added drop wise to the diammonium hydrogen phosphate solution with constant stirring (700rpm) at room temperature. As the precipitation proceeds decrease in pH was observed. A thick white precipitate formed was aged for 12 h then filtered, washed with water and dried in an oven at 120 ºC for 12 h. The dried catalyst was calcined at 600 ºC for 4 h.

Catalyst characterization

The X-ray diffraction analysis was carried out using a Rigaku X-ray diffractometer (Model DMAX IIIVC) with Cu-Kα radiation. FTIR measurements were carried out using Shimadzu 8300 as KBr pellet in the range of 4000–400 cm^{-1} region with 4 cm^{-1} resolution averaged over 100 scans. BET surface area was determined using NOVA 1200 Quanta chrome instrument. Prior to N_2 adsorption, the sample was evacuated at 250 °C. To study Ca/P ratio, scanning electron microscopy EDAX was performed on a Leica Stereoscan-440 instrument equipped with a Phoenix EDAX attachment operated at 20 kV, ICP analysis was carried out on ICP AES SPECTRO ARCOS Germany FHS12 instrument. Temperature programmed desorption of ammonia (NH_3-TPD) and CO_2 (CO_2-TPD) was carried out using a Micromeritics Autocue 2910. For TPD measurement 0.1 g of catalyst sample was used. Sample was dehydrated at 500 °C for 1h in 50 mL min^{-1} helium flow and then cooled to 50 °C. Probe gas (5% NH_3 in helium for acidic sites and 10% CO_2 in helium for basic sites) was then adsorbed for 1h in 50 mL min^{-1} flow. The temperature was raised up to 600 °C at a rate of 10 °C/min in 30 mL min^{-1} helium flow. Raman spectra were recorded under ambient conditions on a Lab RAM infinity spectrometer (Horiba-Jobin-Yvon) equipped with a liquid nitrogen detector and a frequency doubled Nd-YAG laser supplying the excitation line at 532 nm with 1-10 mW power. The spectrometer was calibrated using the Si line at 521 cm^{-1} with a spectral resolution of 3 cm^{-1}. Morphological appearance of the samples using scanning electron microscopy (SEM) was performed on a Leica Stereoscan-440 instrument equipped with a Phoenix EDAX attachment operated at 20 kV. ^{31}P NMR analysis was carried out using Bruker 300 MHz, with resonance frequency of 121.49 MHz. The operating field of 7.05 T, the spinning rates of 8 KHz, with 85% H_3PO_4 as reference material and recycle delay of 5.0 s were used during analysis.

Catalyst activity test

Vapour phase dehydration of lactic acid to acrylic acid was carried out using procedure reported previously.[20] In short quartz fixed bed down flow reactor (id-11mm) was charged with catalyst (particle size 20-40 mesh) in the middle section with quartz wool packed in both the ends. Porcelain beads were placed above the catalyst bed in order to preheat the feed. Before catalytic evaluation, the catalyst was preheated at required reaction temperature for 0.5 h under flow of nitrogen (15 mL min^{-1}). The reaction temperature was measured by a thermocouple inserted in the catalyst bed. Lactic acid of required concentration (typically 50% w/w in water) was pumped in to the preheating zone of reactor using peristaltic pump and nitrogen gas as carrier. The reaction products were collected in a cold trap at 8 °C. The reaction mixture was analysed using gas chromatograph (Perkin Elmer) equipped with a FFAP capillary column (50 M X 0.320 mM) and FID detector. The GC was calibrated by external standard method. The formation of CO and CO_2 was confirmed by GC, with molesieve and porapack Q column respectively using TCD detector. The amount of CO_x (CO and CO_2) was estimated based on the yield of acetaldehyde and propionic acid. The mass balance for all the reaction was more than 90%.

The *in-situ* FTIR studies were carried out using previously reported procedure.[20] In a typical experiment lactic acid was adsorbed on CP and CP-3 catalyst at room temperature. The physisorbed lactic acid was removed by drying the catalyst at room temperature for 8 h and the FTIR spectrum was recorded. The adsorbed lactic acid was desorbed at various temperatures to detect the species formed *in-situ* during the reaction. The spectrum of neat catalyst was subtracted to get the spectrum of adsorbed species.

Acknowledgements

VCG acknowledges CSIR New Delhi for Junior Research Fellowship.

Notes and references

[a]*Catalysis Division, CSIR-National Chemical Laboratory, Dr. Homi Bhabha Road, Pune-411008, India.*
[b]*Academy of Scientific and Innovative Research, CSIR, Anusandhan Bhawan, New Delhi-110 001, India. E-mail: sb.umbarkar@ncl.res.in; Fax: (+91)-2025902633/34.*
† Present address: Mojj Engineering Systems Ltd, 15-81/B, MIDC, Bhosari, Pune,India – 411026.

1 M. D. P. V. Wouwe, A. Dewaele, E. Makshina, B. F. Sels, *Energy Environ. Sci.*, 2013,**6**, 1415–1442.
2. P. Maki-Arvela, I. L. Simakova, T. Salmi, D. Yu. Murzin *Chem. Rev.*, 2014, **114**, 1909–1971.
3 T. J. Korstanje, H. Kleijn, J. T. B. H. Jastrzebski, R. J. M. Klein Gebbink, *Green Chem.,* 2013, **15**, 982–988.
4 (a) G. Gunter, D.J. Miller, J.E. Jackson, *J. Catal.,* 1994, **148**, 252–260; (b) G.C. Gunter, R.H. Langford, J.E. Jackson, D.J. Miller*, Ind. Eng. Chem. Res.,*1995, **34,** 974-980; (c) M. S. Tam, G. C. Gunter, R. Craciun, D. J. Miller, J. E. Jackson, *Ind. Eng. Chem. Res.,* 1997, **36**, 3505-3512; (d) M. S. Tam, R. Craciun, D. J. Miller, J.E. Jackson, *Ind. Eng. Chem. Res*., 1998, **37**, 2360-2366.
5 (a)B. Katryniok, S. Paul, F. Dumeignil, *Green Chem.*, 2010, **12**, 1910–1913; (b) Z. Zhai, X. Li, C. Tang, J. Peng, N. Jiang, W. Bai, H. Gao, Y. Liao*, Ind. Eng. Chem. Res,* 2014, dx.doi.org/10.1021/ie500988q.
6 M. Ai, K. Ohdan, *Appl. Catal. A,* 1997, **165**, 461–465.
7 R.D. Cortright, M. Sanchez-Castillo, J.A. Dumesic, *App. Catal. B: Env.,* 2002, **39**, 353–359.
8 R. E. Holmen, *U.S. Pat*. 2859240, 1958.
9 (*a*) R. A. Sawicki, *U.S. Pat.* 4729978, 1988; (*b*) J. Wang, Z. Zhang'Y. Qu, S. Wang, *Ind. Eng. Chem. Res*., 2009, **48**, 9083–9089; (*c*) J-M. Lee, D-W. Hwang, Y. K. Hwang, S. B. Halligudi, J-S.Chang, Y-H. Han, *Catal. Commun.,* 2010, **11**, 1176–1180.
10 C. Paparizos, S. R. Dolhyj, W. G. Shaw, *U.S. Pat.* 4786756, 1988.
11 C. T. Lira, P. J. McCrackin, *Ind. Eng. Chem. Res*., 1993, **32,** 2608–2613.
12 J. Zhang, J. Lin, P. Cen, *Can. J. Chem. Eng*., 2008, **86**, 1047–1053.
13 (a) H. J. Wang, D. H. Yu, P. Sun, J. Yan, Y. Wang, H. Huang,*Catal. Commun*., 2008, **9**, 1799–1803; (b) P. Sun, D. H. Yu, K. Fu, M. Gu, Y. Wang, H. Huang, H. Ying, *Catal. Commun*., 2009, **10**, 1345–1349; (c) Y. Jie, Y. Dinghua, L. Heng, S. Peng, H. He, *J. Rare Earths*, 2010, **28**, 803–806; (d) Y. Jie, Y. Dinghua, S. Peng, H. He, *Chin. J. Catal*., 2011, **32**, 405–411; (e) J. Zhang, Y. Zhao, M. Pan, X. Feng,W. Ji, C-T. Au, *ACS Catal.,* 2011, **1**, 32–41; (f) B. Yan, L-Z. Tao, Y. Liang, B-Q. Xu, 2014, *Chem. Sus. Chem,* 2014, DOI: 10.1002/cssc.201400134.
14 Y. Fan, C. Zhou, X. Zhu *Catal. Rev.*, 2009, **51,** 293–324.
15 E. Blanco, P. Delichere, J.M.M. Millet, S. Loridant, *Catal. Today,* 2014, **226**, 185–191.
16 J. Peng, X. Li, C. Tang W. Bai, *Green Chem*., 2014, **16**,108.
17 J. H. Hong, J-M. Lee, H. Kim, Y. K. Hwang, J-S Chang, S. B. Halligudi, Y-H Han, *App. Catal A: Gen.,* 2011, **396**, 194–200.
18 (a) Y. Matsuuraa, A. Ondaa,, S. Ogob, K. Yanagisawa, *Catal. Today,* 2014, **226, 1,** 192–197; (b) Y. Matsuuraa, A. Ondaa, K. Yanagisawa, *Catal. Comm.,* 2014, **48,** 5–10.
19 B. Yan, Li-Zhi Tao, Y. Liang, Bo-Qing Xu, *ACS Catal.* 2014, DOI: 10.1021/cs500388x.
20 V. C. Ghantani, S. T. Lomate, M. K. Dongare, S. B. Umbarkar, *Green. Chem.,* 2013, **15**, 1211–1217.
21 A. K. Lynn, W. Bonfield, *Acc. Chem. Res.,* **2005,** 38, 202–207.
22 O. Mekmene, S. Quillard, T Rouillon, J.-M. Bouler, M. Piot, F. Gaucheron, *Dairy Sci. Technol*., 2009, **89**, 301–316.
23 H. C. W. Skinner, *Mat. Res. Bull.,* 1970, **5**, 437–448.
24 S. Raynaud, E.Champion, D.Bernache-Assollant, P.Thomas, *Biomater.,* 2002, **23,**1065–1072.
25 A. M. El Kady, K. R. Mohamed, G. T. El-Bassyouni, *Ceramics International*, 2009, **35,** 2933–2942.
26 K-H Chen, M-J Li, W-T Cheng, T. Balic-Zunic, S-Y Lin, *Int. J. Exp. Path*. 2009, **90**, 74–78.
27 T. J. Korstanje, H. Kleijn, J. T. B. H. Jastrzebski, R. J. M. K. Gebbink, *Green Chem*., 2013, **15**, 982–988.
28 E. Lautemann, *Justus Liebigs Ann. Chem.*, 1860, **113**, 217–220.
29 D. Wadley, M. Tam, P. Kokitkar, J. Jackson and D. Miller, J. Catal., 1997, 165, 162–171.
30 J. H. Hong, J.-M. Lee, H. Kim, Y. K. Hwang, J.-S. Chang, S. B. Halligudi and Y.-H. Han, Appl. Catal., A, 2011, 396, 194–200.
31 (a) J. C. Serrano-Ruiz and J. A. Dumesic, ChemSusChem, 2009, 2, 581–586; (b) J. C. Serrano-Ruiz and J. A. Dumesic, Green Chem., 2009, 11, 1101–1104.
32 B. Odell, G. Earlam and D. J. Cole-Hamilton, *J. Organomet. Chem*., 1985, **290**, 241–248.
33 J. Zhang, Y. Zhao, X. Feng, M. Pan, J. Zhao, W. Ji, C-T Au, *Catal. Sci. Technol*., 2014, **4**, 1376–1385.
34 J. Zhang, X. Feng, Y. Zhao, W. Ji, C-T Au, *J. Ind. Eng. Chem.,* 2013 doi.org/10.1016/j.jiec.2013.07.018.
35 C. Tang, J. Pen, G. Fan, X. Li, X. Pu, W. Bai, *Catal. Comm.*2014*,* **43,** 231–234.
36 K. Brow, R.J. Kirkpatrick, G.L. Turner, *J. Non-Crystal Solids*. 1990, **116**, 39–45.